Pergamon

Int. J. Heat Mass Transfer. Vol. 38, No. 4, pp. 761–765, 1995

0017–9310/95 $9.50+0.00

An integral treatment for combined heat and mass transfer by natural convection in a porous medium

A. NAKAYAMA
Department of Energy and Mechanical Engineering, Shizuoka University, Hamamatsu 432, Japan

and

M. A. HOSSAIN
Department of Mathematics, University of Dhaka, Dhaka 1000, Bangladesh

(*Received* 14 *March* 1994 *and in final form* 12 *May* 1994)

INTRODUCTION

Combined heat and mass transfer driven by buoyancy, due to temperature and concentration variations is of practical importance, since there are many possible engineering applications, such as the migration of moisture through the air contained in fibrous insulations and grain storage installations, and the dispersion of chemical contaminants through water-saturated soil. A comprehensive review on the phenomena has been recently provided by Trevisan and Bejan [1].

Bejan and Khair [2] treated one of the most fundamental cases, namely buoyancy-induced heat and mass transfer from a vertical plate embedded in a saturated porous medium. A scale analysis originally suggested by Bejan [3] was introduced to identify four possible regimes depending on the values of buoyancy ratio and Lewis number, and the numerical solutions to the boundary layer equations were obtained for a limited range of the buoyancy ratio.

In this note, we shall revisit the same physical model as Bejan and Khair, and then extend it to the case of arbitrary shape. Highly accurate heat transfer and mass transfer formulae, which cover all ranges of the buoyancy ratio and Lewis number, are obtained by exploiting a simple integral treatment along the lines of Nakayama and Koyama [4]. All possible physical limiting conditions are examined to construct two distinct regime maps for heat transfer and mass transfer, respectively, which subsequently lead to an interesting paradox overlooked in the previous scale analyses, namely that the pure heat transfer formula may hold even when the flow close to the wall is driven by mass transfer, whereas the pure mass transfer formula may hold even when the flow close to the wall is driven by heat transfer.

ANALYSIS

Consider a vertical flat plate embedded in a saturated porous medium (see Fig. 1). The surface of the plate is maintained at a constant temperature T_w, higher than its ambient temperature T_e, and at the same time the concentration of a certain chemical species decreases from C_w at the wall to C_e sufficiently away from the wall. Under the usual boundary layer approximations, the continuity equation, the Boussinesq approximated Darcy's law, the heat and mass transfer equations are given by

$$\frac{\partial u}{\partial x}+\frac{\partial v}{\partial y}=0 \tag{1}$$

$$\frac{\mu}{K}u=\rho g\beta(T-T_e)+\rho g\beta_c(C-C_e) \tag{2}$$

$$u\frac{\partial T}{\partial x}+v\frac{\partial T}{\partial y}=\alpha\frac{\partial^2 T}{\partial y^2} \tag{3}$$

and

$$u\frac{\partial C}{\partial x}+v\frac{\partial C}{\partial y}=D\frac{\partial^2 C}{\partial y^2} \tag{4}$$

where u, v, T and C are the volume-averaged velocity components, temperature and concentration, respectively. μ and ρ are the solution density and viscosity, K is the permeability of the porous medium, and g is the gravitational acceleration. Furthermore, α and D are the equivalent thermal and mass diffusivity of the saturated porous medium, respectively,

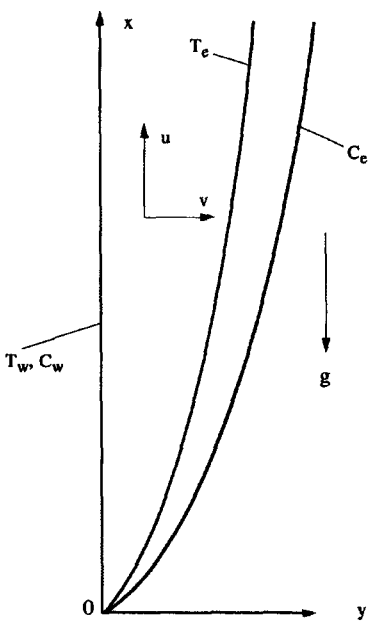

Fig. 1. Physical model and its boundary layer coordinate system.

NOMENCLATURE

A, A_c	shape factors, defined in equation (10a) and (10b)
C	concentration
D	equivalent mass diffusivity of the fluid-saturated porous medium
E	shape factor, defined in equation (10c)
g	acceleration due to gravity
K	intrinsic permeability of the porous media
Le	Lewis number
N	buoyancy ratio, defined in equation (11)
Nu_x	local Nusselt number
Ra_x	local Rayleigh number
Sh_x	local Sherwood number
T	temperature
u, v	Darcian or superficial velocity components
x, y	boundary layer coordinates.

Greek symbols

α	equivalent thermal diffusivity of the fluid-saturated porous medium
β	coefficient of thermal expansion
β_c	coefficient of concentration expansion
δ	arbitrary length scale for thermal boundary layer
ζ	boundary layer thickness ratio, defined in equation (10d)
μ	fluid viscosity
ρ	fluid density.

Subscripts

e	ambient
w	wall.

whereas β and β_c are the thermal expansion and concentration expansion coefficients, respectively. The boundary conditions for the velocity, temperature and concentration are

$$y = 0: \quad v = 0 \quad T = T_w \quad C = C_w \tag{5a}$$

$$y = \infty: \quad u = 0 \quad T = T_e \quad C = C_e. \tag{5b}$$

The energy equation (3) and the constituent conservation equation (4) can be integrated together with the continuity equation (1), using the boundary conditions given by equations (5) as

$$\frac{d}{dx}\int_0^\infty u(T-T_e)\,dy = -\alpha\left.\frac{\partial T}{\partial y}\right|_{y=0} \tag{6}$$

$$\frac{d}{dx}\int_0^\infty u(C-C_e)\,dy = -D\left.\frac{\partial C}{\partial y}\right|_{y=0}. \tag{7}$$

Substituting the Darcy's law given by equation (2) into the foregoing integral equations, and assuming that the temperature and concentration profiles are similar, we transform equations (6) and (7) into

$$A\frac{\rho Kg\beta(T_w-T_e)}{\mu}\frac{d\delta}{dx} = \alpha\frac{E}{\delta} \tag{8}$$

$$A_c\frac{\rho Kg\beta(T_w-T_e)}{\mu}\frac{d\delta}{dx} = D\zeta\frac{E}{\delta} \tag{9}$$

where

$$A = \int_0^\infty \left(\frac{T-T_e}{T_w-T_e} + N\frac{C-C_e}{C_w-C_e}\right)\frac{T-T_e}{T_w-T_e}\,d\left(\frac{y}{\delta}\right) \tag{10a}$$

$$A_c = \int_0^\infty \left(\frac{T-T_e}{T_w-T_e} + N\frac{C-C_e}{C_w-C_e}\right)\frac{C-C_e}{C_w-C_e}\,d\left(\frac{y}{\delta}\right) \tag{10b}$$

$$E = -\frac{\delta}{T_w-T_e}\left.\frac{\partial T}{\partial y}\right|_{y=0} \tag{10c}$$

and

$$\zeta = \frac{T_w-T_e}{C_w-C_e}\frac{\left.\frac{\partial C}{\partial y}\right|_{y=0}}{\left.\frac{\partial T}{\partial y}\right|_{y=0}}. \tag{10d}$$

δ is an arbitrary scale for the thermal boundary thickness, whereas ζ is its ratio to the concentration boundary layer thickness. N is the buoyancy ratio defined as

$$N = \frac{\beta_c(C_w-C_e)}{\beta(T_w-T_e)} \tag{11}$$

such that $N = 0$ for thermal-driven flow and infinite for mass-driven flow.

We assume exponential temperature and concentration profiles as follows:

$$\frac{T-T_e}{T_w-T_e} = \exp\left(-\frac{y}{\delta}\right) \tag{12a}$$

and

$$\frac{C-C_e}{C_w-C_e} = \exp\left(-\zeta\frac{y}{\delta}\right) \tag{12b}$$

such that

$$A = \frac{1+\zeta+2N}{2(1+\zeta)} \quad A_c = \frac{2\zeta+(1+\zeta)N}{2\zeta(1+\zeta)} \quad \text{and} \quad E = 1 \tag{13a–c}$$

Substituting these shape factors into equations (8) and (9), we integrate the equations to obtain two distinct expressions for δ^2 as

$$(\delta/x)^2\,Ra_x = \frac{4(1+\zeta)}{1+2N+\zeta} = \frac{4\zeta^2(1+\zeta)}{\{N+(2+N)\zeta\}Le} \tag{14}$$

where $Ra_x = \rho Kg\beta(T_w-T_e)x/\alpha\mu$ is the local Rayleigh number and $Le = \alpha/D$ is the Lewis number. The foregoing two expressions for $(\delta/x)^2\,Ra_x$ can be combined to give the following cubic algebraic equation for determining the boundary layer thickness ratio ζ as

$$\zeta^3 + (1+2N)\zeta^2 - \{(2+N)Le\}\zeta - N\,Le = 0. \tag{15}$$

As ζ is determined from the foregoing equation, the local Nusselt number and Sherwood number of our primary interest are given by

$$Nu_x = -\frac{x}{T_w-T_e}\left.\frac{\partial T}{\partial y}\right|_{y=0} = \frac{x}{\delta} = 0.5\left(\frac{1+2N+\zeta}{1+\zeta}\right)^{1/2} Ra_x^{1/2} \tag{16}$$

and

$$Sh_x = -\frac{x}{C_w-C_e}\left.\frac{\partial C}{\partial y}\right|_{y=0} = \zeta\frac{x}{\delta}$$

$$= 0.5\zeta\left(\frac{1+2N+\zeta}{1+\zeta}\right)^{1/2} Ra_x^{1/2}$$

$$= 0.5\left\{\frac{N+(2+N)\zeta}{1+\zeta}\right\}^{1/2} Le^{1/2} Ra_x^{1/2}. \quad (17)$$

The accuracy acquired in the foregoing approximate expressions may be examined by comparing the approximate heat and mass transfer results against the exact solution [5] for the two limiting cases of pure thermal-driven flow (i.e. $N = 0$) and pure mass-driven flow (i.e. $N \to \infty$), as follows:

$$\left.\frac{Nu_x}{Ra_x^{1/2}}\right|_{N=0} = \left.\frac{Sh_x}{(Ra_x\, Le\, N)^{1/2}}\right|_{N\to\infty} = \begin{cases} 0.500: \text{approximate} \\ 0.444: \text{exact} \end{cases} \quad (18)$$

Our approximate expressions given by equations (16) and (17) tend to overestimate heat and mass transfer rates under these physical limiting conditions. It is not unusual to have an error of 10% or more, depending on the assumed profile. (Note that, if a linear profile [4] is used instead, we would have underestimated the transfer rates.) However, the situation can be remedied by adjusting the multiplicative constant, namely, replacing 0.5 by 0.444. Thus, we propose the following final approximate formulae:

$$Nu_x = 0.444\left(\frac{1+2N+\zeta}{1+\zeta}\right)^{1/2} Ra_x^{1/2} \quad (19a)$$

and

$$Sh_x = 0.444\zeta\left(\frac{1+2N+\zeta}{1+\zeta}\right)^{1/2} Ra_x^{1/2} \quad (19b)$$

where the boundary layer thickness ratio ζ is given by equation (15). Following Merkin [6] and Nakayama and Koyama [4], the above results may be translated to the general case of arbitrary shape (see ref. [4] for the details). The generalized expressions run as

$$Nu_x = 0.444\left(\frac{1+2N+\zeta}{1+\zeta}\right)^{1/2} (Ra_x/I)^{1/2} \quad (20a)$$

and

$$Sh_x = 0.444\zeta\left(\frac{1+2N+\zeta}{1+\zeta}\right)^{1/2} (Ra_x/I)^{1/2} \quad (20b)$$

where

$$I(x) = \int_0^x r^2 \sin\phi\, dx/(xr^2 \sin\phi) \quad (20c)$$

and

$$r(x) = \begin{cases} 1: \text{plane body} \\ \displaystyle\int_0^x \cos\phi\, dx: \text{axisymmetric body.} \end{cases} \quad (20d)$$

The generalized coordinate x measures the distance around the body surface from the lower stagnation point, whereas $\phi(x)$ is the angle between the outward normal to the body and the downward vertical, such that the local Rayleigh number is defined as $Ra_x = \rho K g \sin\phi\beta(T_w - T_e)x/\alpha\mu$. The functions $I(x)$ for various geometries may be found in ref. [4].

While any numerical integration scheme encounters numerical difficulties, as either N or Le becomes extremely small or large, the present integral treatment, as will be shown shortly, is free from such difficulties associated with the physical limiting conditions.

RESULTS AND DISCUSSION

In Table 1, the heat and mass transfer results generated by the present approximate formulae, equations (19a) and (19b), are compared with those of the exact solution furnished by Bejan and Khair [2]. Fairly good agreement can be seen between the approximate and exact solutions for an entire range, and, hence, the present approximate formulae may well suffice for fast and accurate estimation of heat and mass transfer rates. The boundary layer thickness ratio ζ [defined by equation (10d)] is plotted in Fig. 2 in terms of its reciprocal, following Bejan and Khair [2]. For the case of $N = 0$, a simple closed form expression for ζ can be obtained from the algebraic equation (15) as

$$Nu_x/Sh_x = 1/\zeta = \frac{(1+8Le)^{1/2}+1}{4Le} \quad \text{for } N = 0. \quad (21)$$

It is also interesting to note that the cubic equation (15) yields $\zeta = 1$ for $Le = 1$ such that our approximate formulae reduce to

Table 1. Local Nusselt and Sherwood numbers

		$Nu_x/Ra_x^{1/2}$		$Sh_x/Ra_x^{1/2}$	
N	Le	Exact	Present	Exact	Present
4	1	0.992	0.993	0.992	0.993
	2	0.899	0.896	1.431	1.436
	4	0.798	0.797	2.055	2.072
	6	0.742	0.743	2.533	2.562
	8	0.707	0.707	2.936	2.976
	10	0.681	0.681	3.290	3.341
	100	0.521	0.519	10.521	10.792
1	1	0.628	0.628	0.628	0.628
	2	0.593	0.591	0.930	0.937
	4	0.559	0.557	1.358	1.383
	6	0.541	0.539	1.685	1.728
	8	0.529	0.528	1.960	2.019
	10	0.521	0.520	2.202	2.276
	100	0.470	0.469	7.139	7.539
0	1	0.444	0.444	0.444	0.444
	2	0.444	0.444	0.683	0.693
	4	0.444	0.444	1.019	1.053
	6	0.444	0.444	1.275	1.332
	8	0.444	0.444	1.491	1.568
	10	0.444	0.444	1.680	1.776
	100	0.444	0.444	5.544	6.061

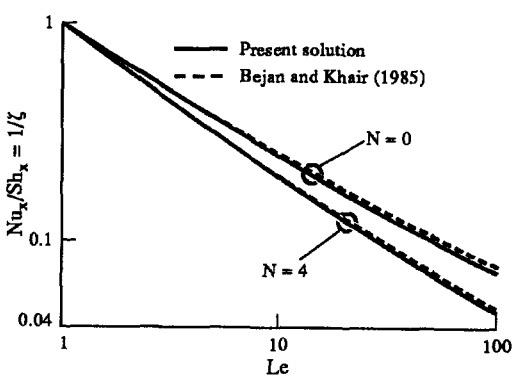

Fig. 2. Boundary layer thickness ratio.

$$Nu_x/Ra_x^{1/2} = Sh_x/Ra_x^{1/2} = 0.444(1+N)^{1/2} \quad \text{for } Le = 1. \tag{22}$$

The effects of Le and N on the heat and mass transfer rates are shown in Figs. 3 and 4, following Lai and Kulacki [7] for a wide range of Le. Again, excellent agreement is confirmed between the present approximate solution and the exact solution of Lai and Kulacki.

A careful examination of the cubic equation (15) reveals that there are three distinct asymptotic cases depending on which two terms (out of the four terms) in equation (15) are predominant. Thus, the following asymptotic results for ζ, depending on the values of N and Le:

$$\zeta = \{(2+N)Le\}^{1/2} \quad \text{for} \quad Le \gg \frac{(1+2N)^2}{2+N} \tag{23a}$$

which is the case where the first and third terms are predominant;

$$\zeta = \left(\frac{N\,Le}{1+2N}\right)^{1/2} \quad \text{for} \quad Le \ll \frac{N(1+2N)}{(2+N)^2} \tag{23b}$$

which is the case where the second and fourth terms are predominant; and

$$\zeta = \frac{2+N}{1+2N}Le \quad \text{for} \frac{N(1+2N)}{(2+N)^2} \ll Le \ll \frac{(1+2N)^2}{2+N} \tag{23c}$$

which is the case where the second and third terms are predominant.

These asymptotic results are illustrated in Fig. 5, using a log N–log Le plane. The curves dividing the regimes may well be approximated by the two straight lines for $Le = 1$ and $Le = N$.

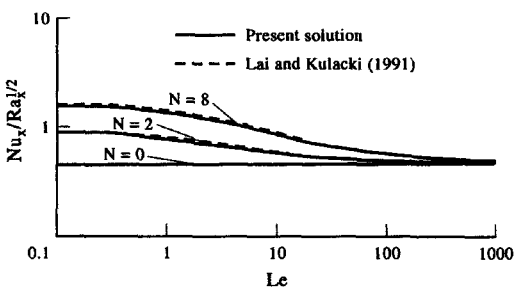

Fig. 3. Heat transfer results.

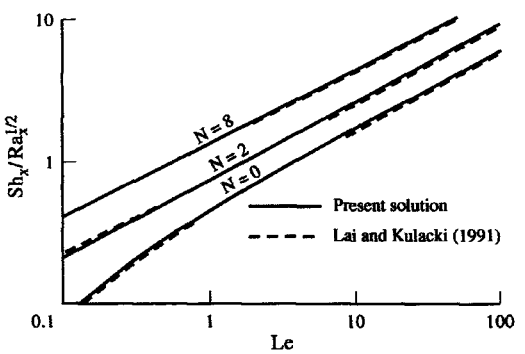

Fig. 4. Mass transfer results.

The foregoing results, when substituted into equations (19a) and (19b), yield various asymptotic expressions for Nu_x and Sh_x, depending on the N and Le values, as follows:

Asymptotic results for heat transfer:

$$\text{Regime I } (N \ll 1 \text{ or } Le \gg N): \quad Nu_x = 0.444Ra_x^{1/2} \tag{24a}$$

$$\text{Regime II } (1 \ll Le \ll N): \quad Nu_x = 0.888(Ra_x\,N/Le)^{1/2} \tag{24b}$$

$$\text{Regime III } (N \gg 1 \text{ and } Le \ll 1): \quad Nu_x = 0.628(Ra_x\,N)^{1/2}. \tag{24c}$$

Asymptotic results for mass transfer:

$$\text{Regime I } (N \gg 1 \text{ or } Le \ll N): \quad Sh_x = 0.444(Ra_x\,N\,Le)^{1/2} \tag{25a}$$

$$\text{Regime II } (N \ll Le \ll 1): \quad Sh_x = 0.888Le\,Ra_x^{1/2} \tag{25b}$$

$$\text{Regime III } (N \ll 1 \text{ and } Le \gg 1): \quad Sh_x = 0.628(Ra_x\,Le)^{1/2}. \tag{25c}$$

Thus, we should bear in mind that the line dividing the regimes I and II is the $Le = N$ line rather than the $N = 1$ line, as implied in scaling arguments by Bejan [3] and Bejan and Khair [2]. Let us consider the regime $1 \ll N \ll Le$ in the heat transfer map (Fig. 6). In this regime, the flow in the vicinity of the wall is driven essentially by mass transfer, since $1 \ll N$. Yet, the pure heat transfer formula (24a) remains valid in this regime, because the the concentration boundary layer thickness is so thin that the heat transfer rate is virtually unaffected by mass transfer. A similar consideration can be made for the regime $Le \ll N \ll 1$ in the mass transfer map (Fig. 7), arriving at another paradoxical conclusion that the pure mass transfer formula (25a) holds even when the flow close to the wall is driven by heat transfer. These paradoxical conclusions, which have been overlooked in the previous scale analyses [2, 3], can be appreciated as we re-examine the $Nu_x/Ra_x^{1/2}$ curves shown in Fig. 3, with reference to the heat transfer regime map (Fig. 6). As we increase Le along a constant N line with N fixed at some value greater than unity (say $N = 8$) in the heat transfer

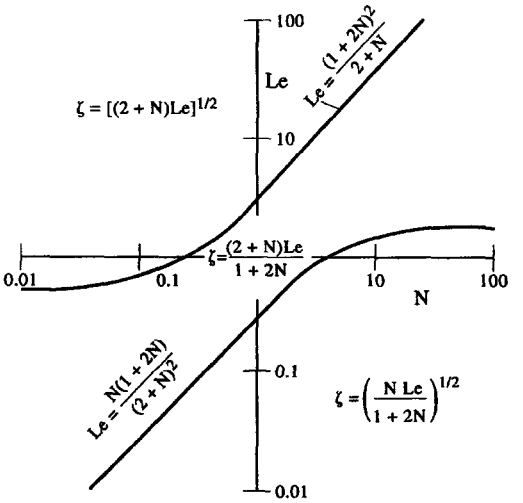

Fig. 5. Regime map for boundary layer thickness ratio.

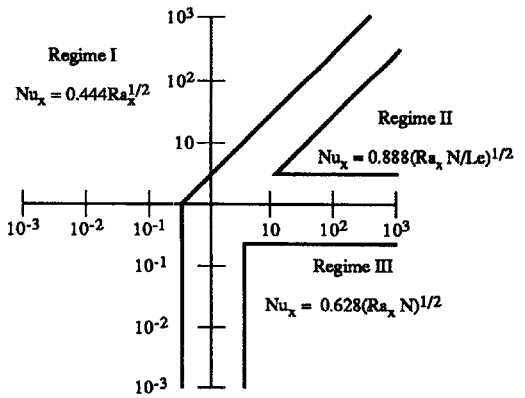

Fig. 6. Regime map for heat transfer.

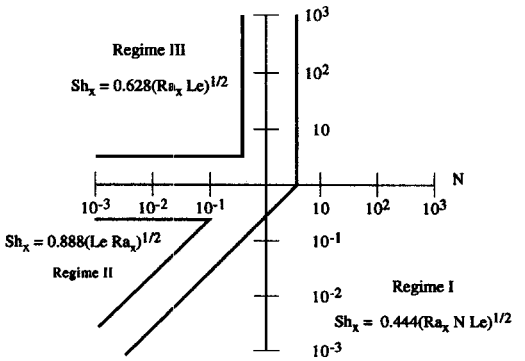

Fig. 7. Regime map for mass transfer.

regime map, we proceed from the regime III, through II and then to I, whereas we stay within the regime I when N is sufficiently lower than unity. Note that the $Nu_x/Ra_x^{1/2}$ curves in Fig. 3 change their slopes correspondingly as we increase Le. A similar observation can be made for the mass transfer regime map.

An integral treatment, such as the present one, remains a powerful means to attack boundary layer problems, since it naturally captures correct asymptotic behaviors, whereas scale arguments are not completely free from a danger of misinterpretation.

REFERENCES

1. O. V. Trevisan and A. Bejan, Combined heat and mass transfer by natural convection in a porous medium, *Adv. Heat Transfer* **20,** 315–352 (1990).
2. A. Bejan and K. R. Khair, Heat and mass transfer by natural convection in a porous medium, *Int. J. Heat Mass Transfer* **28,** 909–918 (1985).
3. A. Bejan, *Convection Heat Transfer*, Chap. 1, pp. 335–338. Wiley, New York (1984).
4. A. Nakayama and H. Koyama, Free convective heat transfer over a nonisothermal body of arbitrary shape embedded in a fluid-saturated porous medium, *Trans. ASME J. Heat Transfer* **109,** 125–130 (1987).
5. P. Cheng and W. J. Minkowycz, Free convection about a vertical plate embedded in a saturated porous medium with application to heat transfer from a dike, *J. Geophys. Res.* **82,** 2040–2044, (1977).
6. J. H. Merkin, Free convection boundary layers on axisymmetric and two-dimensional bodies of arbitary shape in a saturated porous medium, *Int. J. Heat Mass Transfer* **22,** 1461–1462 (1979).
7. F. C. Lai and F. A. Kulacki, Coupled heat and mass transfer by natural convection from vertical surfaces in porous media, *Int. J. Heat Mass Transfer* **34,** 1189–1194